Inter–decadal modulations in the dynamic state of the Kuroshio Extension system: 1905–2017

Bo Qiu (bo@soest.hawaii.edu), S. Chen, and N. Schneider
University of Hawaii at Manoa, Hawaii, USA

Introduction

After separating from the Japanese coast at 36^{o}N, 141^{o}E, the Kuroshio enters the open basin of the North Pacific, where it is renamed the Kuroshio Extension (KE) (Figure 1). Free from the constraint of coastal boundaries, the KE has been observed to be an eastward-flowing inertial jet accompanied by large-amplitude meanders and energetic pinched-off eddies. Compared to its upstream counterpart south of Japan, the KE is accompanied by a stronger southern recirculation gyre (RG) that increases the KE's eastward volume transport to more than twice the maximum Sverdrup transport (~60Sv) in the subtropical North Pacific Ocean, enhancing its nonlinear nature as a western boundary current extension.

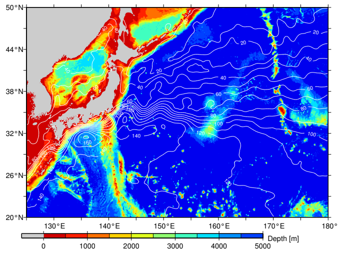

Figure 1: Bottom topography and mean dynamic height (CLS13).

An important feature emerging from the past 25-year satellite altimeter measurements is that the KE system exhibits clearly-defined decadal modulations between a stable and an unstable dynamic state. As shown in Figure 2, the KE paths were relatively stable in 1993-1995, 2002-2005 and 2010-2017. In contrast, spatially convoluted paths prevailed during 1996-2001 and 2006-2009.

By clarifying the relationship and physical processes between the basinscale wind forcing and the KE dynamic state over the altimeter era, we hindcast the KE dynamic state going back to 1905 with the use of ECMWF reanalysis wind stress product. It is found that the low-frequency KE variability modulated in the past century in connection with the mid-1920s, mid-1940s, and mid-1970s' climatic regime shifts in the Aleutian Low pressure system.

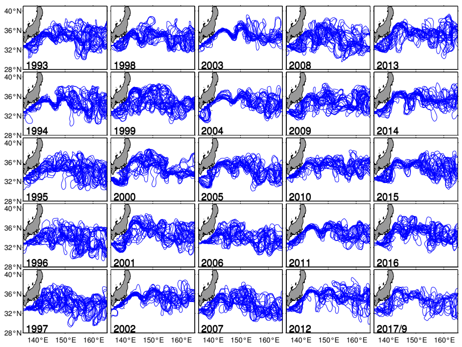

Figure 2: Semi-monthly KE paths in 1993-2016 based on satellite altimeter data, revealing the stabel vs. unstalbe dynamical states of the KE sysmtem.

KE Index during the Satellite Era

To succinctly summarize the time-varying dynamical state of the KE system, Qiu et al. (2014) introduced the KE index defined as average of the variance-normalized time series of negative of the upstream KE path length, the KE's intensity, latitudinal position, and negative of its southern RG intensity (Fig. 3). A positive KE index, thus defined, indicates a stable dynamical state and a negative KE index, an unstable dynamical state. Dominance of the decadal modulation in the KE system is easily discernible in this time series (Fig. 3e).

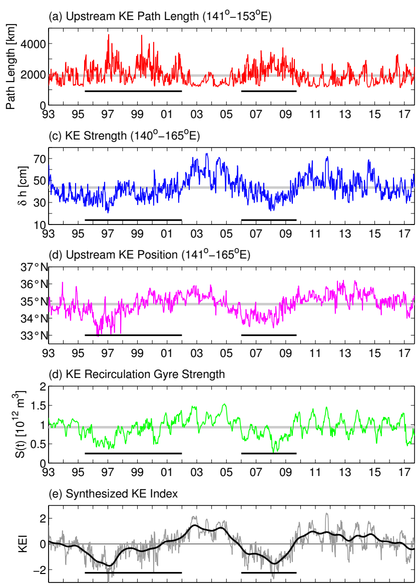

Figure 3: Time series of (a) upstream KE path length integrated from 140°E to 153°E, (b) SSH difference across the KE jet averaged from 140°E to 165°E, (c) latitudinal position of the KE averaged from 141°E to 158°E, (d) intensity of the KE recirculation gyre, and (e) KE index time series synthesized from the four dynamic quantities shown in a-d. Grey lines denote the mean values averaged over the period of analysis. Thick black lines denote the periods when the KE is in an unstable dynamic state.

A regression analysis reveals that the KE index defined by the 4 dynamical properties can be favorably represented by the sea surface height (SSH) signals inside the KE's southern RG region of 31^o-36^{o}N and 140^o-165^{o}E (red lines in Fig. 4b). The linear correlation coefficient between the two red and thick (thin) black lines in Fig. 4b is as high as 0.97 (0.85). Physically, this high correlation is of little surprise because the large-scale KE variability is closely entwined to the dynamical state of its southern RG and the RG's variability is well represented by its regional SSH signals. On a practical level, this makes exploration of the KE dynamical state be equivalent to examination of the SSH signals in the key region of the KE's southern RG.

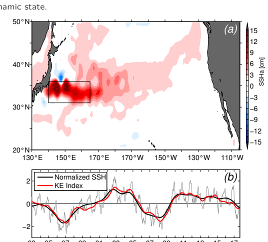

Figure 4: (a) Regression map between the KE index shown in (b, red line) and the SSH anomaly time series in the North Pacific Ocean. All results are based on the satellite altimeter measurements. (b) KE index time series synthesized from the four dynamic quantities shown in Fig. 3, And time series of the SSH anomalies averaged in the region 31°–36°N and 140°–165°E (i.e., the rectangular box in c).

Support from NASA Ocean Surface Topography Science Team (OSTST) Is Acknowledged.

Rossby Wave Model and PDO-related Wind Forcing

The large-scale, wind-induced, SSH variability in a midlatitude ocean is governed by the long-wave linear vorticity equation:

$$\frac{\partial \eta}{\partial t} - c_R \frac{\partial \eta}{\partial x} = -\frac{g'}{g} w_{Ek}, \tag{1}$$

where η is the SSH anomaly of our interest, c_R the long baroclinic Rossby wave speed, g the gravity constant, g' the reduced gravity, and w_{Ek} the anomalous Ekman pumping velocity. By solving Eq. (1) as an initial value problem, we can write the solution for η as follows:

$$\eta(x,y,t) = \eta\left[x + c_R(t-t_o), y, t_o\right] - \frac{g'}{g}\int_{t_o}^{t} w_{Ek}\left[x + c_R(t-t'), y, t'\right] dt', \tag{2}$$

where t_o is the initialization time and $t > t_o$. As the KE index is closely related to the SSH anomalies (Fig. 4b), Eq. (2) constitutes a useful dynamic framework to explore the relationship between PDO-related wind forcing and KE system variability (See Figs. 6c and 6d).

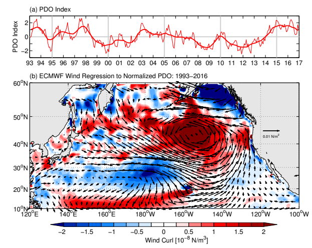

Figure 5: (a) PDO index in recent decades. (b) ECMWF interim wind stress and curl that are regressed to the PDO index. Center of PDO wind forcing is in the eastern half of Pacific basin.

Transitions between the KE's two dynamical states are caused by the basin-scale wind stress curl forcing in the eastern North Pacific related to the Pacific decadal oscillations (PDOs) (Fig. 5). Specifically, when the central North Pacific wind stress curl anomalies are positive (i.e. positive PDO phase), enhanced Ekman flux divergence generates negative local SSH anomalies in 170^o-150^{o}W along the southern RG latitude. As these wind-induced negative SSH anomalies propagate westward as baroclinic Rossby waves into the KE region after a delay of 3-4 years (Fig. 6b), they weaken the zonal KE jet, leading to an unstable (i.e., negative index) state, of the KE system with a reduced recirculation gyre and an active eddy kinetic energy field. The negative, anomalous wind stress curl forcing during the negative PDO phase, on the other hand, generates positive SSH anomalies through the Ekman flux convergence in the eastern North Pacific. After propagating into the KE region in the west, these anomalies stabilize the KE system by increasing the KE transport and by shifting its position northward, leading to a positive index state.

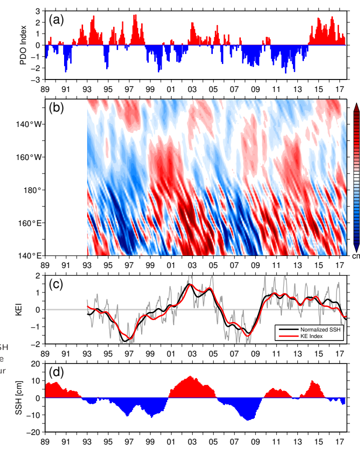

Figure 6: a) Time series of Pacific decadal oscillation (PDO). (b) SSH anomalies along the zonal band of 32^o-34^{o}N from the AVISO satellite altimeter data. (c) Time series of the KE index synthesized from four dynamical properties (red line) versus the normalized SSH anomalies averaged in 31^o-36^{o}N and 140^o-165^{o}E (black lines); here, the thin black line denotes the weekly time series and the thick black line the low-pass filtered time series. (d) SSH anomalies in the 31^o-36^{o}N and 140^o-165^{o}E box predicted by the 1.5-layer reduced-gravity model forced by the ECMWF Interim wind stress data.

KE Index over the Past Century

Use of the SSH signals in the southern RG box as a proxy for the KE dynamical state allows us to explore the KE index variations beyond the satellite altimetry era. To achieve this, we merge the ECMWF reanalysis wind stress product ERA-20C (available from 1900 to 2010) and ERA-Interim (available from 1979 to June 2017) and force the 1.5-layer reduced-gravity model. Fig. 7a shows the model-derived SSH changes in the KE's southern RG box of 31^o-36^{o}N and 140^o-165^{o}E. For comparison and serving as an independent check, we plot in Fig. 7b the time series of surface dynamic height calculated from the historical, objectively-analyzed, T/S data compiled by Ishii et al. (2006) in the same southern RG box from 1945 to 2012. Because the available T/S data is confined to the upper ocean of 1,500m, the amplitude of the T/S-based KE index is, on average, about half that derived from the wind-forced 1.5-layer reduced-gravity model. However, the observed phase changes of the KE index agree well with those predicted by the wind-forced model hindcast. The linear correlation coefficient between the two time series in 1960-2012 is 0.82, as compared to 0.74 during the overlapping period of 1945-2012.

Both Figs. 7a and 7b reveal that the low-frequency modulation of the KE dynamical state is not confined to the last two decades during which we had satellite-based SSH information to capture the detailed evolution of the KE system. To examine how the dominant period of the century-long KE index has modulated over the past century, we plot in Fig. 7c the wavelet power spectrum for the KE index time series shown in Fig. 7a. Large-amplitude decadal changes can be seen to persist after the mid-1970s. From mid-1940s to mid-1970s, the KE index appears to have two dominant periods: one in the 15 20-year band and the other in the 4 6-year band. In between the mid-1920s and mid-1940s, the KE index appears to be dominated by the 10 15-year fluctuations and prior to the mid-1920s, Fig. 7c indicates that the predominant period of the time-varying KE index falls in between 6 and 10 years.

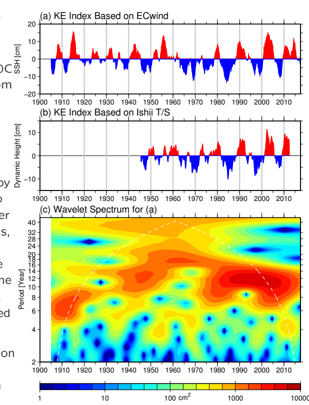

Figure 7: (a) KE index time series based on the SSH anomalies in the 31^o-36^{o}N and 140^o-165^{o}E box predicted by the 1.5-layer reduced-gravity model forced by the merged ERA-20C and Interim wind stress data. (b) KE index time series based on the SSH anomalies in the 31^o-36^{o}N and 140^o-165^{o}E box calculated from the historical T/S data of Ishii et al. (2006). Notice the difference from (a) in y-axis scale. (c) Wavelet power spectrum for the time series of (a).

Summary

- KE dynamic state (i.e. EKE level, path latitude, and jet/RG strengths) is dominated by decadal variations.
- SSH anomalies in 31-36^{o}N , 140-165^{o}W prodive a good proxy fro the decadally-varying KE system; its variations are dictated by basin-wide PDO-related wind forcing.
- The mid-1920s, mid-1940s, and mid-1970s marked the three 20th-century climatic regime shifts in the Aleutian Low pressure system over the North Pacific Ocean. Our results in Fig. 7 clearly indicate that these regime shifts in the atmospheric forcing field exert a significant impact upon the frequency content of the time-varying KE system.